Heteroatom Chemistry
Volume 13, Number 4, 2002

Phenylhydrazine–Borane Adduct—Characterized in the Solid State and in Solution

Bernd Wrackmeyer,[1] Angelo G. Giumanini,[2] Alberto Gambi,[2]
Giancarlo Verardo,[2] Gastone Gilli,[3] and Valerio Bertolasi[3]

[1]*Laboratorium für Anorganische Chemie, University of Bayreuth, D-95440 Bayreuth, Germany*

[2]*Department of Chemical Sciences and Technologies, University of Udine, I-33100 Udine UD, Italy*

[3]*Centre of Diffrattometric Structure, University of Ferrara, I-44100 Ferrara FE, Italy*

Received 22 November 2001

ABSTRACT: *The 1:1 phenylhydrazine–borane adduct, obtained from phenylhydrazine and sodium borohydride in acidic solution, was investigated by IR, NMR spectroscopy, and MS spectrometry. Ab initio MO calculations indicated the isomer in which the boron center is attached to the primary amino group as the more stable. This forecast was confirmed by solution-state ^{1}H, ^{11}B, ^{13}C, and ^{15}N NMR spectroscopy, in agreement with the molecular structure in the solid state determined by X-ray analysis.* © 2002 Wiley Periodicals, Inc. Heteroatom Chem 13:366–372, 2002; Published online in Wiley Interscience (www.interscience.wiley.com). DOI 10.1002/hc.10049

INTRODUCTION

Although synthesis and properties of borane–amine adducts are well documented, very scant and sometimes contradictory information is available on hydrazine–borane complexes. Doubts still persist to which nitrogen the BH_3 group is attached in the 1:1 complexes, $RN_2H_3{-}BH_3$ or $R_2NNH_2{-}BH_3$ [1]. Methylhydrazine yields a mixture of $MeNHNH_2{-}BH_3$ and $MeNH(BH_3)NH_2$ adducts in an approximately 10:1 molar ratio [2]. In the case of the phenylhdrazine-1-boraadamantane adduct, it has been proposed that the boron atom is linked to the NH_2 group [3], whereas it was suggested that triarylboranes, depending on their bulkiness, are linked either to the NH or to the NH_2 group of methylhydrazine [4]. The phenylhydrazine–borane adduct has been used several times as a reducing agent [5]; however, it has never been properly characterized. It has been inferred [6], on the basis of an alleged stronger basicity of the NH_2 group, that the phenylhydrazine BH_3 adduct **1** (Scheme 1) bears the BH_3 group on the NH_2 as in **1a**, but nucleophilic reactions are usually linked to the other nitrogen atom. By and large, the solid adducts which are obtained from the reaction solutions containing the respective hydrazine and the borane or its precursor may be the combined result of dynamic equilibria and differing solubility. The present work is intended to clarify the situation for the phenylhydrazine–borane adduct both in solution and in the solid state.

EXPERIMENTAL

Infrared Spectra

IR spectra were obtained with a Bruker Vector 22 Fourier Transform spectrometer in the range

---

Correspondence to: Angelo G. Giumanini or Bernd Wrackmeyer; e-mail: angelo.giumanini@dstc.uniud.it; b.wrack@uni-bayreuth.de.

Contract grant sponsor: CNR funds, Italy.
Contract grant sponsor: MURST.
Contract grant sponsor: Morton International S.p.A. (now Rohm and Haas).
Contract grant sponsor: Deutsche Forschungsgemeinschaft.
Contract grant sponsor: The Fonds der Chemischen Industrie.

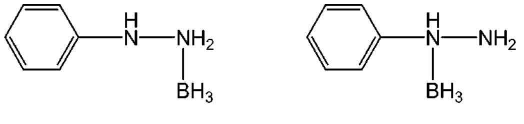

1a **1b**

SCHEME 1

4000–400 cm^{-1} at a resolution of 2 cm^{-1}. The sample intimately mixed with dried KBr and then pressed in an evacuated die under high pressure gave rise to transparent discs. The sample concentration was about 1% (see Fig. 1).

Synthesis of Phenylhydrazine–Borane Adduct **1**

Sodium borohydride (powder, 130 mmol) was partly dissolved at room temperature in freshly distilled phenylhydrazine (27 mmol). Complete dissolution was achieved by the addition of H_2O (30 ml, neither any heat nor gas evolution was observed). The obtained solution was slowly added to 3 M aqueous H_2SO_4 (initially 10 ml, then as much as needed to keep the pH below 4; further additions to a total of 27 ml, 8.33 mmol) keeping the mixture of the strongly exothermal, gas-evolving reaction below 30°C by external cooling. The homogeneous mixture was stirred for 2 h at room temperature, then neutralized with $NaHCO_3$ to pH 8 and extracted with CH_2Cl_2. Evaporation of the solvent gave yellowish crystals, which were recrystallized as snow white crystals from hexane-CH_2Cl_2, mp 113.4°C [6], yield: 57%. (Melting points were determined with an automatic Mettler (Mod. FP61) instrument and are not corrected). The pure compound **1** is readily soluble in alcohols, ethers, CH_2Cl_2, $CHCl_3$, AcOEt, and CH_3CN; sparingly soluble in benzene; and insoluble in aliphatic hydrocarbons. It proved to be stable towards acids and bases, whereas it did not withstand the required GC conditions, and yielded free phenylhydrazine.

Gas Chromatography and Mass Spectrum

GC–MS analyses were performed with a Fisons TRIO 2000 gas chromatograph–mass spectrometer, working in the positive ion at 70- and 20-eV electron impact mode. Spectra were recorded in the range 35–450 mu.

NMR Data

^{1}H (200 and 500 MHz), ^{11}B (160.5 MHz), ^{13}C (50.3 and 125.8 MHz), and ^{15}N NMR spectra (50.7 MHz) were recorded on Bruker AC-F 200 and DRX 500 spectrometers using saturated solutions of **1** in 5-mm tubes at room temperature if not stated otherwise (see Table 1). Chemical shifts are given relative to TMS [^{1}H, ^{13}C (using the signal of the partially or fully deuterated solvent)], external

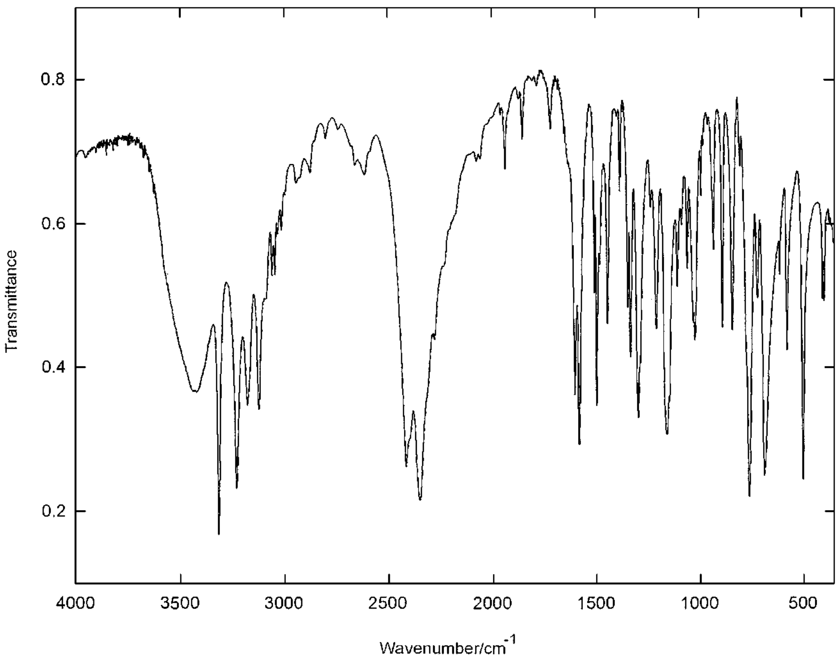

FIGURE 1 IR spectrum of **1** in KBr disc.

TABLE 1 ^{1}H, ^{11}B, ^{13}C and ^{15}N NMR Data of Phenylhydrazine-Borane (**1a**)

	NH_2[a]	*NH*[b]	*BH_3*[c]	*ortho*	*para*	*meta*
$\delta^{1}H$ (CD_2Cl_2)	5.81	5.33	1.78	6.81	7.05	7.35
(C_6D_6/CD_2Cl_2)[d]	4.65	4.88	2.00	5.95	6.20	6.90
(CD_3CN)	6.30	5.60	1.71	6.83[e]	6.90[e]	7.28
$\delta^{13}C$ (CD_2Cl_2)[f]	–	–	–	114.2	123.1	130.0
(C_6D_6/CD_2Cl_2)[d]	–	–	–	114.1	122.7	129.8
(CD_3CN)	–	–	–	115.0	122.0	130.0
$\delta^{11}B$ (CD_2Cl_2)	–	–	−17.9[c]	–	–	–
$\delta^{15}N$ (CD_2Cl_2)	−287.7	−245.2	–	–	–	–

[a] $^{1}J(^{15}N, ^{1}H) = 76.1$ Hz; $^{3}J(^{1}H, N, N, ^{1}H) = 4.2$ Hz; $^{3}J(^{1}H, N, B, ^{1}H) = 4.2$ Hz.
[b] $^{1}J(^{15}N, ^{1}H) = 82.7$ Hz; $^{3}J(^{1}H, N, N, ^{1}H) = 4.2$ Hz.
[c] $^{1}J(^{11}B, ^{1}H) = 115.0$ Hz; $h_{1/2} = 74$ Hz (20°C).
[d] Mixture 95/5.
[e] Multiplet from $\delta^{1}H = 6.83$–6.90.
[f] $\delta^{13}C$(*ipso*) 148.3 (in CD_2Cl_2), 146.3 (in C_6D_6/CD_2Cl_2), 147.8 (in CD_3CN).

Et_2O—BF_3 with $\delta^{11}B = 0$ for $\Xi(^{11}B) = 32.083971$ MHz, and external neat $MeNO_2$ with $\delta^{15}N = 0$ for $\Xi(^{15}N) = 10.136767$ MHz.

X-ray Structural Analysis [7]

Crystal Data. $C_6H_{11}BN_2$, M = 121.98, orthorhombic, space group $Pca2_1$ (no. 29), $a = 7.675(3)$, $b = 13.319(5)$, $c = 7.402(3)$ Å, $U = 756.7(5)$ Å^3, $\lambda = 0.71073$ Å, $Z = 4$, $D_c = 1.07$ g cm^{-3}, $\mu = 0.64$ cm^{-1}, $F(000) = 264$.

Data Collection, Processing and Refinement. CAD-4 diffractometer, $\omega/2\theta$ scan mode, graphite-monochromated Mo–Kα radiation, 981 unique reflections measured ($2 < \theta < 28°$) giving 588 observed reflections with $I > 2\sigma(I)$, corrected for Lorentz and polarization effects. Solution was obtained by direct methods using SIR92 [8] system of programs. Full-matrix least-square refinement on F^2, using SHELX-97 [9], with all non-hydrogen atoms anisotropic and hydrogens isotropic, was effected. Final R (observed reflections) = 0.072.

Table 2 reports bond distances and angles of **1**, and Fig. 2 shows an ORTEP [10] view of the molecule.

RESULTS AND DISCUSSION

Infrared Spectrum and Computational Part

The infrared spectrum of the solid complex PhN_2H_3—BH_3 (**1**) dispersed in KBr (Fig. 1) exhibits a broad intense band for the stretching vibration of a hydrogen-bonded NH group, followed in the same range by sharp bands for the NH_2 group (symmetric and asymmetric stretchings) and the aromatic CH stretching bands, for which also two well-separated bands appear. The perfectly isolated bands at 2415 and 2348 cm^{-1} for the BH_3^- stretching modes in which the boron octet is complete are the strongest in the whole spectrum. The rather strong bands at 1603 and 1581 cm^{-1}, in the region of the aromatic ring stretching modes, may be attributed to the NH and NH_2 deformations. The BH_3^- deformations can be localized around 1100 cm^{-1}, where also the NH_2 rocking mode is expected. The NH, NH_2 wagging mode is represented by the two sharp bands at 764 and 689 cm^{-1}. In this region, the BN dative bond should also give rise to an absorption band according to previous observations on borane amines [11].

TABLE 2 Bond Distances (Å) and Bond Angles (degrees) for **1a**[a]

Bond distances	
B1—N1	1.586(6) [1.658]
N1—N2	1.424(5) [1.434]
N2—C1	1.413(5) [1.407]
C1—C2	1.365(6)
C1—C6	1.384(6)
C2—C3	1.392(7)
C3—C4	1.369(8)
C4—C5	1.353(8)
C5—C6	1.364(8)
Bond angles	
B1—N1—N2	112.8(3) [112.3]
N1—N2—C1	116.0(3) [120.3]
N2—C1—C2	122.1(4) [122.0]
N2—C1—C6	118.6(4) [118.7]
C2—C1—C6	119.2(4)
C1—C2—C3	120.0(4)
C2—C3—C4	120.1(5)
C3—C4—C5	119.2(5)
C4—C5—C6	121.6(5)
C1—C6—C5	119.8(5)

[a] Some calculated (HRB3LYP/6-311++G) structural parameters are given in brackets.

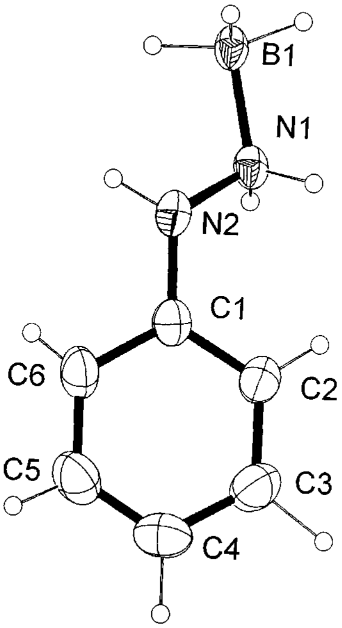

FIGURE 2 An ORTEP view of **1** showing the thermal ellipsoids at 30% probability.

Ab initio molecular orbital calculations were carried out using the Gaussian 98 [12] program package. Calculations were performed at LCAO–MO–SCF restricted Hartree–Fock (HF) level and by using the density functional theory (DFT) in the form of Becke's three parameters functional hybrid method [13] in combination with Lee, Yang, and Parr correlation functional [14] (B3LYP). In preliminary calculations both the **1a** and **1b** gas-phase structures were optimized at HF/6-31G, and these structures were further optimized at the B3LYP/6-311++G levels of theory. The results indicate that structure **1a** is more stable by 24.6 kJ mol^{-1} at B3LYP/6-311++G level, and this corresponds to the experimental NMR data in solution and also to the results of the X-ray structural analysis (vide infra). In contrast, the analogous calculations for $MeNHNH_2{-}BH_3$ and $MeNH(BH_3){-}NH_2$ indicate that the latter adduct is slightly more stable (5 kJ mol^{-1}) than the former. Except for the longer distance B–N (1.658 Å), the calculated structural parameters for **1a** in the gas phase are close to those determined by X-ray structural analysis in the solid state (see Table 2). In the case of the ammonia–borane adduct $H_3N{-}BH_3$, the B3LYP/6-311++G calculated distance B–N (1.671 Å) is also longer than the distance experimentally determined (1.565 Å [15]). The Gaussian 98 implementation of the gauge-independent atomic orbital (GIAO) method for calculating nuclear magnetic shielding tensors at both HF and DFT levels [16] was successfully employed (vide infra).

E.I. Mass Spectrometry

The 70-eV electron impact mass spectrum obtained by vaporizing **1** at room temperature directly into the ion source does not exhibit the parent peak for $C_6H_{11}{}^{11}BN_2$ at 122, but a cluster at 120-117, an evidence for a cascade of hydrogen atom losses. In the range between 17 and 120 mu the most intense peak appears at 108 mu, which corresponds to the mass of phenylhydrazine whose EI-fragmentation closely resembles the lower mass part of the spectrum.

NMR Data

All NMR data of **1** are given in Table 1, and Fig. 3 shows representative ^{1}H and ^{13}C NMR spectra. The NMR data of **1** support the proposed composition in solution. The δ^{13}C data obtained for solutions of **1** in three different solvents [CD_3CN, CD_2Cl_2, and C_6D_6/CD_2Cl_2 (95/5)] are almost identical. They can be interpreted to represent structure **1a**, considering the shielding of ^{13}C(o) and ^{13}C(p) with respect to benzene [17] as a result of CN(pp)π interactions which would be absent in the case of **1b**. The δ^{11}B value of **1** (−17.9) is clearly in the range known for borane adducts of primary amines [18]. Although there is a pronounced solvent dependence of the δ^1H values, fast interconversion of the potential isomers **1a** and **1b**, depending on the polarity of the solvent, is rather unlikely, taking into account the constant δ^{13}C values. Final evidence for the structure **1a** in solution is provided by close inspection of ^{1}H(NH) and ^{1}H(NH_2) resonance signals. The latter is shown in Fig. 4, enhanced in order to show the ^{15}N satellites. These appear as a doublet [$^1J(^{15}N, {}^1H) = 76.1$ Hz] of quintets, since the coupling constants $^3J(^1H, N, N, {}^1H)$ and $^3J(^1H, N, B, {}^1H)$ are of the same magnitude (4.2 ± 0.2 Hz). For comparison, in $H_3N{-}BH_3$ and $MeNH_2{-}BH_3$, the magnitude of coupling constants $^3J(^1H, N, B, {}^1H) = 3.8 \pm 0.2$ Hz has been measured [19]. The ^{15}N satellites of the ^{1}H(NH) resonance signal are a doublet [$^1J(^{15}N, {}^1H) = 82.7$ Hz] of triplets [$^3J(^1H, N, N, {}^1H) = 4.2$ Hz]. This evidence was further corroborated by the $^1H/^{15}N$ HMQC shift correlation [20,21] which shows that the ^{15}N NMR signal at $\delta - 287.7$ belongs to the $NH_2{-}BH_3$ group, whereas the signal at $\delta - 245.2$ must be assigned to the NH group.

Chemical shifts δ^{11}B, δ^{13}C, and δ^{15}N of **1a** and **1b** were calculated by the GIAO method [12,16] employing the B3LYP/6-311++G level of theory (Table 3); both calculations have been performed using the B3LYP/6-311++G optimized geometry. The data for **1b** did not agree at all with the experimental values, whereas the data calculated for **1a** showed

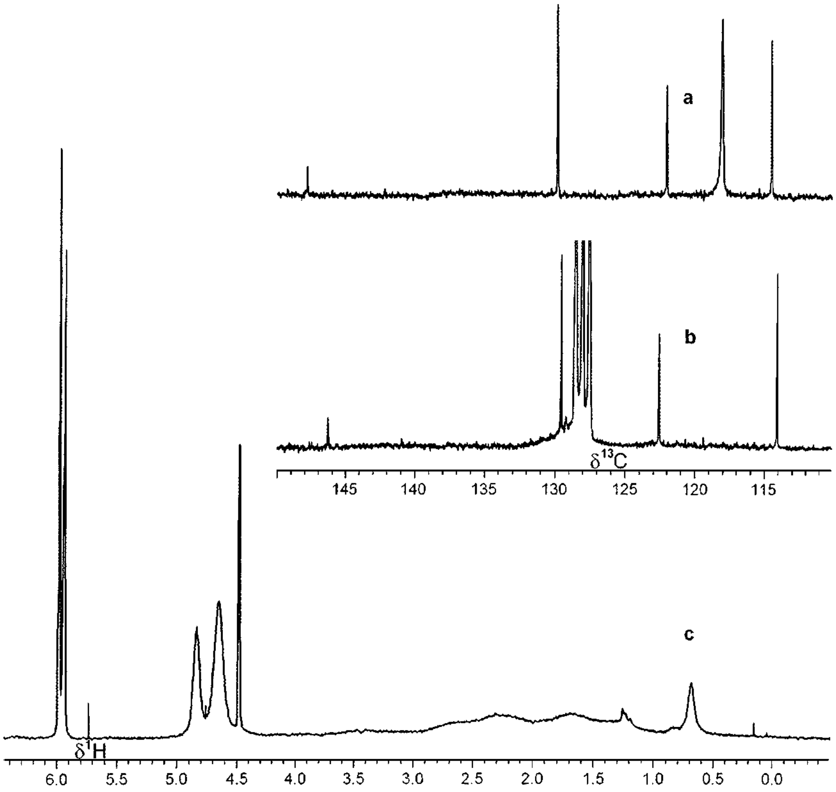

FIGURE 3 Representative 50.3 MHz ^{13}C (a, b) and 200 MHz ^{1}H NMR spectra (c) of **1** at room temperature. (a) 50.3 MHz $^{13}C\{^{1}H\}$ NMR in CD_3CN; (b) 50.3 MHz $^{13}C\{^{1}H\}$ NMR in C_6D_6/CD_2Cl_2 (95/5); (c) 200 MHz ^{1}H NMR spectrum in C_6D_6/CD_2Cl_2 (95/5). The broad $^{1}H(NH)$ and $^{1}H(NH_2)$ resonances at δ 4.65 and δ 4.88 and the extremely broad $^{1}H(BH_3)$ resonance at δ 2.00 are clearly visible.

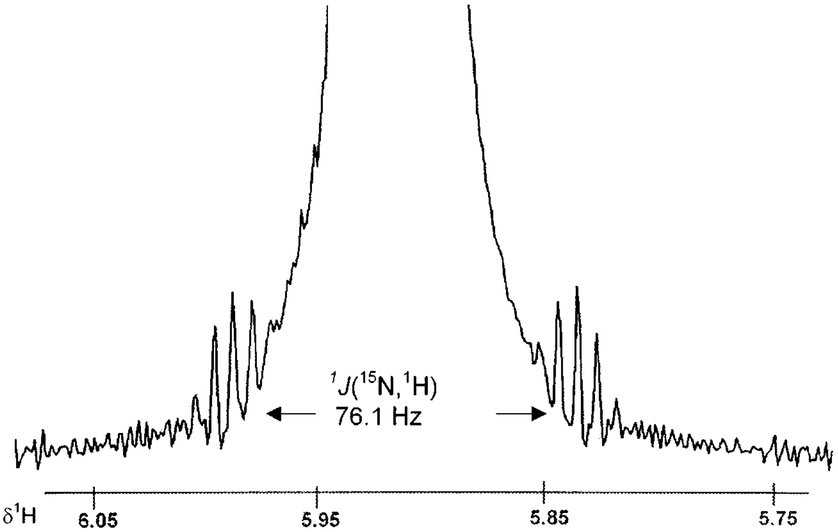

FIGURE 4 500 MHz ^{1}H NMR spectrum of **1** in CD_2Cl_2 at 20°C; the part of the $^{1}H(NH_2)$ region is shown and enhanced in order to display the ^{15}N satellites. The satellite pattern clearly indicates the presence of the fragment —NH_2—BH_3 with coupling constants $^{1}J(^{15}N, ^{1}H)$ as given and $^{3}J(^{1}H, N, N, ^{1}H) \approx {}^{3}J(^{1}H, B, N, ^{1}H) = 4.2$ Hz.

TABLE 3 Comparison of Experimental and Calculated Chemical Shifts

	B3LYP/6-311++G	*Experimental*
$\delta^{11}B^{a}$	−18.4	−17.9
$\delta^{13}C^{b}$ (*ipso*)	153.2	148.3
ortho	116.0^{c}	114.2
para	127.9	123.1
meta	137.1^{c}	130.0
$\delta^{15}N^{d}$ (NH_2—BH_3)	−306.5	−287.7
(NH)	−261.6	−245.2

[a] $\delta^{11}B$ (B_2H_6) = 18.0; B3LYP/6-311++G: $\sigma(B_2H_6) = +87.6$.
[b] $\delta^{13}C$ (TMS) = 0; B3LYP/6-311++G: σ(TMS) = +190.1.
[c] Mean value.
[d] $\delta^{15}N$ ($NH_{3\text{gaseous}}$) = −399.3; B3LYP/6-311++G: $\sigma(NH_3)$ = +268.4.

a consistent trend or reasonable agreement with experimental $\delta^{13}C$ and $\delta^{15}N$ values. The calculated and experimental $\delta^{11}B$ data are in close agreement. The calculation of ^{11}B nuclear shielding has proved to be a fairly reliable tool for many boron compounds [22]. For comparison, the molecular structure and NMR data for H_3N—BH_3 were calculated at the B3LYP/6-311++G level and gave satisfactory agreement with experimental data [$\delta^{11}B - 19.6$ (calc.), −22.3 (exp. [18]); $\delta^{14}N - 364.1$ (calc.), −370 (exp. [18])].

X-ray Analysis

The molecular structure of **1** is shown in Fig. 2, and relevant structural parameters are listed in Table 2. The N1 and B1 atoms are not in the mean plane of the phenyl ring, the torsion angles C2—C1—N2—N1, C6—C1—N2—N1 and C1—N2—N1—B1 having values of 33.5(5)°, −150.4(4)°, and 166.2(3)° (calculated for the gas phase: 22.8, −158.0°, and 156.8°; the surroundings of N(2) are also pyramidal: calculated sum of bond angles is 350.2°). The torsion angles are such that B1 is more displaced by the phenyl ring [0.720(5) Å] than N1 [0.547(2) Å]. The most interesting feature of the molecule concerns the donor–acceptor binding of BH_3 to the terminal N1 atom at a B1—N1 distance of 1.586(6) Å. In this process the planar BH_3 becomes pyramidal with an average N1—B1—H angle of 105° (calculated for the gas phase: 104.1°, 104.5°, 105.6°) similar to the average of the three B1—N1—N2 and B1—N1—H of some 112°. The observed B1—N1 distance can be compared well with the value of 1.565 Å in ammonia–borane [15], 1.564 Å in hydrazine–borane [23], and 1.600 Å in ethylenediamine–bis(borane) [24]. From a CSD (Cambridge Structural Database) [25] search, it has been found that this distance is longer for the complexes with secondary amines (in the range 1.61–1.62 Å) and tertiary amines (in the range 1.61–1.66 Å), in spite of the increasing gas-phase basicity in the series $N_2H_4 < NH_3 < NH_2R < NHR_2 < NR_3$. This fact can be interpreted in terms of Pearson's hard–soft acid–base theory [26]. The BH_3 Lewis acid is unable to take advantage of the increased basic strength of the hard nitrogen bases because of its intrinsic softness and, in this situation, the repulsion forces prevail and the B—N distance is found to increase with the bulkiness of the substituents at the nitrogen. The same steric reasons could explain the observed preferred attack of BH_3 at the relatively unhindered N1 instead of the more crowded N2 atom, irrespective of their relative basicities. The structure **1a** of the solid adduct is thus coincidental with that of **1** in solution. The molecules in the crystals appear to be held together both by a dipole–dipole interaction in the region of the BH bonds and van der Waals interactions between stacked phenyl groups.

REFERENCES

[1] (a) Gayaso, E.; Gayaso, M. An Fis 1970, 66, 233; (b) Durig, J. R.; Chatterjee, S.; Casper, J. M.; Odom, J. D. J Inorg Nucl Chem 1972, 34, 1805.

[2] Zakharov, V. V.; Lagodzinskaya, G. V.; Nikitin, V. S.; Eselson, B. M.; Zhigach, A. F.; Nechiporenko, G. N. Zh Fiz Khim 1975, 49, 804.

[3] Mikhailov, B. M.; Smirnov, V. N.; Smirnova, O. D.; Kasparov, V. A.; Lagutkin, N. A.; Mitin, N. I.; Zubairov, M. M. Khim-Farm Zh 1979, 13, 35.

[4] Lapkin, I. I.; Yushakova, G. A.; Ukhanov, S. E.; Zueva, V. I.; Nikoshina, T. A. Zh Obshch Khim 1979, 49, 2286.

[5] Fleming, R. A. US Patent, 2992061 196 10711, 1961; Chem Abstr 55:127733; (b) Kametani, T.; Kigasawa, K.; Hiragi, M.; Wagatsuma, N.; Kohagizawa, T.; Inoue, H. Yakugaku Zasshi 1982, 102, 241.

[6] Baumgarten, R. J.; Henry, M. C. J Org Chem 1964, 29, 3400.

[7] Crystallographic data (excluding structure factors) for the structure reported in this paper have been deposited with the Cambridge Crystallographic Data Centre as supplementary publication no. CCDC-174567 (**1**). Copies of the data can be obtained free of charge on application to CCDC, 12 Union Road, Cambridge CB2 1EZ, UK [fax (internet.): +44 (0)1223/336033; e-mail: deposit@ccdc.cam.ac.uk].

[8] Altomare, A.; Cascarano, G.; Giacovazzo, C.; Guagliardi, A.; Burla, M. C.; Polidori, G.; Camalli, M. J Appl Cryst 1994, 27, 435.

[9] Sheldrick, G. M. SHELXL97. Program for Crystal Structure Refinement, University of Göttingen, Germany, 1997.

[10] Johnson, C. K. ORTEPII. Report ORNL-5138, Oak Ridge National Laboratory, Oak Ridge, 1976.

[11] (a) Goubeau, J.; Ricker, E. Z. Anorg Allgem Chem 1961, 310, 123; (b) Taylor, R. C.; Cluff, C. L. Nature (London) 1958, 182, 390.

[12] Frisch, M. J.; Trucks, G. W.; Schlegel, H. B.; Scuseria, G. E.; Robb, M. A.; Cheeseman, J. R.; Zakrzewski, V. G.; Montgomery, J. A., Jr.; Stratmann, R. E.; Burant, J. C.; Dapprich, S.; Millam, J. M.; Daniels, A. D.; Kudin, K. N.; Strain, M. C.; Farkas, O.; Tomasi, J.; Barone,

V.; Cossi, M.; Cammi, R.; Mennucci, B.; Pomelli, C.; Adamo, C.; Clifford, S.; Ochterski, J.; Petersson, G. A.; Ayala, P. Y.; Cui, Q.; Morokuma, K.; Malick, D. K.; Rabuck, A. D.; Raghavachari, K.; Foresman, J. B.; Cioslowski, J.; Ortiz, J. V.; Baboul, A. G.; Stefanov, B. B.; Liu, G.; Liashenko, A.; Piskorz, P.; Komaromi, I.; Gomperts, R.; Martin, R. L.; Fox, D. J.; Keith, T.; Al-Laham, M. A.; Peng, C. Y.; Nanayakkara, A.; Challacombe, M.; Gill, P. M. W.; Johnson, B.; Chen, W.; Wong, M. W.; Andres, J. L.; Gonzalez, C.; Head-Gordon, M.; Replogle, E. S.; Pople, J. A. Gaussian 98, Revision A.9, Gaussian, Inc., Pittsburgh, PA, 1998.

[13] Becke, A. D. J Chem Phys 1993, 98, 5648.

[14] Lee, C.; Yang, W.; Parr, R. G. Phys Rev B 1988, 37, 785.

[15] Bühl, M.; Steinke, T.; Schleyer, P.R.V.; Boese, R. Angew Chem 1991, 103, 1179; Angew Chem Int Ed Engl 1991, 30, 1160.

[16] Cheeseman, J. R.; Trucks, G. W.; Keith, T. A.; Frisch, M. J. J Chem Phys 1996, 104, 5497.

[17] Ewing, D. F. Org Magn Reson 1970, 12, 499.

[18] Nöth, H.; Wrackmeyer, B. In Nuclear Magnetic Resonance Spectroscopy of Boron Compounds, NMR—Basic Principles and Progress; Diehl, P.; Fluck, E.; Kosfeld, R. (Eds.); Springer: Berlin, 1978; Vol. 14, pp. 284–286.

[19] Wrackmeyer, B. unpublished heteronuclear $^{1}H\{^{11}B\}$ double resonance experiments.

[20] Bax, A.; Sparks, S. W.; Torchia, D. A. In Methods of Enzymology; Oppenheimer, N. J.; James, T. L. (Eds.); Academic Press: San Diego, 1989; Vol. 176, Part A, p. 134.

[21] Wrackmeyer, B.; Kupce, E.; Köster, R.; Seidel, G. Magn Reson Chem 1992, 30, 393.

[22] (a) Bühl, M.; Schleyer, P. V. R. J Am Chem Soc 1992, 114, 477; (b) Hermanek, S.; Hnyk, D.; Bühl, M. In Advances in Boron Chemistry; Siebert, W. (Ed.); The Royal Society of Chemistry: Cambridge, 1977; pp. 30–37; (c) Onak, T. In The Borane, Carborane, Carbocation Continuum; Casanova, J. (Ed.); Wiley: New York, 1998; pp. 247–258.

[23] Andrianov, V. I.; Atovmyan, L. O.; Golovina, N. I.; Klitskaya, G. A. Zh Strukt Khim 1967, 8, 303.

[24] Ting, H. Y.; Watson, W. H.; Kelly, H. C. Inorg Chem 1972, 11, 374.

[25] Allen, F. H.; Bellard, S.; Brice, M. D.; Cartwright, B. A.; Doubleday, A.; Higgs, H.; Hummelink, T.; Hummelink-Peters, B. G.; Kennard, O.; Motherwell, W. D. S.; Rodgers, J. P.; Watson., D. G. Acta Crystallogr, Sect B 1979, 35, 2331.

[26] Pearson, R. G. J Am Chem Soc 1963, 85, 3533.